Int. J. Heat Mass Transfer. Vol. 36, No. 16, pp. 3949–3956, 1993
Printed in Great Britain

0017-9310/93 $6.00 + 0.00

Transient cooling of a finite cylindrical medium in the rarefied cold environment

SEUNG WOOK BAEK and TAIK YOUNG KIM
Korea Advanced Institute of Science and Technology, Aerospace Engineering Department, 373-1 Gusung-dong, Yusung-ku, Taejon, Korea

and

JOON SIK LEE
Seoul National University, Mechanical Engineering Department, 56-1 Sinlim-dong, Kwanak-ku, Seoul, Korea

(*Received* 3 *December* 1992 *and in final form* 21 *April* 1993)

Abstract—Unsteady cooling problem with conduction and radiation is examined here for a finite cylindrical medium that is exposed to the rarefied cold environment. To solve the energy conservation equation and radiative transfer equation, the finite difference technique with the Crank–Nicolson scheme and the discrete ordinates method were chosen respectively. A parametric study was performed to find the effects of optical diameter, conduction-to-radiation parameter and scattering albedo. Cooling characteristics were discussed through the mean temperature and emittance of the medium. It has been greatly affected by those parameters.

1. INTRODUCTION

IN THIS study a transient radiative cooling of finite cylindrical semitransparent medium, when simultaneously combined with conduction, is examined under rarefied cold environment. Its application lies in a number of engineering applications such as the cooling of high-temperature porous ceramic insulating media, ceramic coatings at high temperature, formation of crystals in an outer space environment and waste heat dissipation technique for an orbiting space power plant. Resulting from its engineering importance, many papers have been reported for different geometries. One-dimensional transient cooling for slab [1–9], cylindrical [10, 11] and spherical [12, 13] configurations respectively was explored under various conditions. Two-dimensional rectangular medium has been also investigated by Siegel [14, 15], but only a radiative cooling was taken into consideration.

Recently, Siegel [5] proposed that there exists a fully developed state for the radiative cooling case alone. When the medium initially at uniform high temperature is exposed to a rarefied cold and black surroundings, the temperature near the boundary rapidly decreases. Therefore, the medium temperature loses its uniformity and a steep temperature gradient is established in the boundary layer. Concurrently, the emittance of the medium is expeditiously dropping from its initial value. But as the transient cooling proceeds further, the temperature distribution is steadily developing to a certain profile that is thereafter maintained. When this similar temperature profile is established, the emittance of the radiating medium is held constant throughout the remaining cooling period. Siegel called this constant emittance state the fully developing condition. Due to the similarity of the temperature profile, the time and space wise coordinates can be decoupled from the other. Using this feature, Siegel introduced the separation of variable technique to efficiently obtain good results [6, 11, 14]. In the case that the conduction is involved in redistributing the thermal energy, the fully developing temperature profile cannot be resolved, since the conduction continuously makes the internal temperature distribution uniform. Therefore the emittance of the medium decreases in the cooling period and then it is recovered to its initial value corresponding to the new uniform temperature [9].

Unsteady multidimensional thermal problems, including radiation, have been numerically studied by a few researchers because of their mathematical difficulties and requirement of large computational storage and time. A latest development of computer performance makes their numerical analysis practical and efficient. Simultaneously, many competent methods were devised and improved to solve the radiative transfer equation. Among others the discrete ordinates method was developed by Carlson and Lathrop [16] for application to the neutron transport equations. Since then, it was applied to various engineering problems [17–20]. The discrete ordinates method, conceptually, belongs to a family of flux models, but corrects lack of accuracy and efficiency of the conventional flux models, which were verified by others [18–19].

NOMENCLATURE

A, V_P dimensionless area and volume for computational cell depicted in Fig. 1
Ar aspect ratio, D/L
c_p specific heat
D, L diameter and length
I dimensionless intensity, $\hat{I}/n^2\sigma\hat{T}_i^4$
n refractive index
N conduction-to-radiation parameter, $\lambda\beta/4n^2\sigma\hat{T}_i^3$
q dimensionless heat flux, $\hat{q}/n^2\sigma\hat{T}_i^4$
t dimensionless time, $4\beta n^2\sigma\hat{T}_i^3\hat{t}/\rho c_p$
T dimensionless temperature, $\hat{T}/\hat{T}_i$
T_m dimensionless mean temperature defined in equation (5)
r, z dimensionless radial and axial coordinates, $\hat{r}/D$, $\hat{z}/L$.

Greek symbols
β extinction coefficient, $\kappa+\sigma_0$
ε_m mean emittance defined in equation (6)
θ, ϕ angular coordinates depicted in Fig. 1
κ absorbing coefficient
λ thermal conductivity
μ, η, ξ directional cosines defined in Fig. 1
ρ density
σ Stefan–Boltzmann constant
σ_0 scattering coefficient
τ_D optical diameter, βD
ω_0 scattering albedo, σ_0/β
Ω solid angle.

Subscripts and superscripts
C conduction
e, w, n, s faces of the computation cell
P centre of computation cell
R radiation
T total
$\hat{}$ dimensional quantity.

In this paper, a transient cooling of a finite cylindrical semitransparent medium is numerically analyzed in axisymmetry, when it is brought up to the rarefied black-body environment. The thermal energy inside the medium is transmitted by both radiation and conduction. The effect of thermal properties including optical diameter, conduction-to-radiation parameter and scattering albedo on the transient cooling characteristics is examined. The new aspect to this study is as follows; the inclusion of axisymmetric treatment of radiation in the cylindrical medium; inclusion of conduction inside the medium. Since the conduction is taken into consideration, there would be no similarity in the long-time solution as mentioned above.

2. ANALYSIS

2.1. *Governing equations*

Consider a finite cylindrical semitransparent medium of diameter D and length L. It is initially at a uniform temperature $\hat{T}_i$ and instantaneously placed in a rarefied black surroundings at a very low temperature. The medium emits the energy by radiation at the boundary and the thermal energy is internally redistributed by radiation and conduction. Because only the radiative loss to the surroundings is assumed, there would be no conductive or convective energy transfer to the surroundings. The incoming radiation from the surroundings is neglected due to its very low temperature.

By defining the dimensionless variables listed in the nomenclature, the transient energy conservation equation can be expressed as follows:

$$\frac{\partial T}{\partial t}=\frac{N}{\tau_D^2}\left\{\frac{1}{r}\frac{\partial}{\partial r}\left(r\frac{\partial T}{\partial r}\right)+Ar^2\frac{\partial^2 T}{\partial z^2}\right\}-\frac{1-\omega_0}{4}\left\{4T^4-\int_{\Omega=4\pi} I\,\mathrm{d}\Omega\right\} \quad (1)$$

where the first two terms on the right hand side indicate two-dimensional conduction and the last two terms the divergence of radiative heat flux.

Energy can be conducted into a surface layer from the inside, but this energy cannot be radiated exactly from the surface layer to the outside, for the boundary of the medium joining the rarefied surroundings is externally insulated with regard to the conduction portion of the energy transfer. The surface layer is semitransparent so that the energy from within the region can pass through boundaries only by radiation. Therefore, the boundary conditions at the left, right and circumferential surfaces for the equation (1) are zero temperature gradient. The symmetric condition is imposed at the axisymmetric axis. Since all the temperature is non-dimensionalized with respect to its initial value, the initial condition of temperature is unity.

By balancing the radiative energy emitted, absorbed and scattered, the dimensionless radiative transfer equation can be given as

$$\frac{1}{\tau_D}\left[\frac{\mu}{r}\frac{\partial(rI)}{\partial r}-\frac{1}{r}\frac{\partial(\eta I)}{\partial\phi}+Ar\xi\frac{\partial I}{\partial z}\right]+I=\frac{1-\omega_0}{\pi}T^4+\frac{\omega_0}{4\pi}\int_{\Omega'=4\pi}\Phi(\Omega'\to\Omega)I\,\mathrm{d}\Omega' \quad (2)$$

where Φ is the scattering phase function. In the present

analysis Φ is set to 1 which corresponds to the isotropic scattering. It is assumed that there is no incoming radiative intensity from outside the boundary.

2.2. *Supplementary equations*

The directional total heat flux in each radial or axial direction consists of conductive and radiative heat fluxes as follows

$$q_r^T = q_r^C + q_r^R = -\frac{4N}{\tau_D}\frac{\partial T}{\partial r} + \int_{\Omega=4\pi} \mu I \, d\Omega$$

$$q_z^T = q_z^C + q_z^R = -\frac{4ArN}{\tau_D}\frac{\partial T}{\partial z} + \int_{\Omega=4\pi} \xi I \, d\Omega. \quad (3)$$

As previously mentioned, there is only radiative heat loss toward the outside environment through the boundary. The instantaneous total heat loss per unit area can be integrated to the following form:

$$q_{loss} = \frac{1}{1+Ar/2}\left\{2Ar\int_0^{1/2}(|q_z^R|_{z=0} + |q_z^R|_{z=1})r \, dr + \int_0^1 |q_r^R| \, dz\right\}. \quad (4)$$

The instantaneous mean temperature across the medium can be defined as

$$T_m = \frac{\rho c_p \int_0^L \int_0^{D/2} \hat{T} 2\pi\hat{r} \, d\hat{r} \, d\hat{z}}{\rho c_p \hat{T}_i \pi D^2 L/4} = 8\int_0^1 \int_0^{1/2} Tr \, dr \, dz \quad (5)$$

which implies the ratio of the remaining energy at any time to the initial energy.

By making use of this mean temperature, the transient mean emittance can be formulated as two types,

$$\varepsilon_m = \frac{q_{loss}}{T_m^4}$$

$$\varepsilon_m = -\frac{8\tau_D}{T_m^4(1+Ar/2)}\int_0^1 \int_0^{1/2} \frac{\partial T}{\partial t} r \, dr \, dz. \quad (6)$$

Whereas the former results from considering the heat loss at the boundaries, the latter is defined by calculating the rate of waste of energy in the medium. By nature, they should be identical.

3. NUMERICAL METHOD

To solve the energy conservation equation the finite difference technique with the Crank–Nicolson scheme has been chosen, which is unconditionally stable and has second order accuracy.

The discrete ordinates method considers the radiative transfer equation only in a finite number of directions spanning a full range of the total solid angle 4π. The resulting discrete equation with double subscripts mn, which can be obtained by the direct-differencing technique for angular derivative, can be written as

$$\frac{1}{\tau_D}\left[\frac{\mu_{mn}}{r}\frac{\partial(rI^{mn})}{\partial r} - \frac{1}{r}\frac{\alpha_{mn+1/2}I^{mn+1/2} - \alpha_{mn-1/2}I^{mn-1/2}}{w_{mn}} + Ar\xi_{mn}\frac{\partial I^{mn}}{\partial z}\right] + I^{mn} = \frac{1-\omega_0}{\pi}T^4 + \frac{\omega_0}{4\pi}\sum_{m'}^{m_M}\sum_{n'}^{n_M}\Phi_{m'n'\to mn}w_{m'n'}I^{m'n'};$$

$$m = 1, \ldots, m_M, n = 1, \ldots, n_M \quad (7)$$

where the coefficients $\alpha_{mn+1/2}$ for the angular derivative term are determined from the following recurrence formula:

$$\alpha_{mn+1/2} - \alpha_{mn-1/2} = w_{mn}\mu_{mn} \quad (8)$$

with the initial value of $\alpha_{m1/2} = 0$.

As long as the symmetry and invariance properties of the physical system are to be preserved, the choice of ordinate directions Ω_{mn} and quadratic weighting factor w_{mn} is arbitrary. However, a complete symmetric quadrature is preferred because of its generality [16]. In general there are $N(N+2)$ directions for $N = 2, 4, 6, \ldots$. This N is the accompanying letter of so called S-N discrete ordinate scheme. For the present study 24 directions have been chosen and thus it is called S-4 approximation. But there are only 12 independent directions due to its axisymmetry. Preliminary evaluations revealed that the S-4 approximation is quite adequate in present analysis, for no measurable gain in accuracy was obtained by higher order approximations such as S-6 and S-8. Hence only S-4 approximation is used here. The ordinate directions and quadratic weighting factors are given in Table 1 according to Fiveland [18].

By integrating equation (7) over the control volume

Table 1. The ordinate directions and weighting factors for the S-4 approximation

m	n	μ_{mn}	η_{mn}	ξ_{mn}	w_{mn}
1	1	−0.2959	0.2959	−0.9082	$\pi/3$
1	2	0.2959	0.2959	−0.9082	$\pi/3$
2	1	−0.9082	0.2959	−0.2959	$\pi/3$
2	2	−0.2959	0.9082	−0.2959	$\pi/3$
2	3	0.2959	0.9082	−0.2959	$\pi/3$
2	4	0.9082	0.2959	−0.2959	$\pi/3$
3	1	−0.9082	0.2959	0.2959	$\pi/3$
3	2	−0.2959	0.9082	0.2959	$\pi/3$
3	3	0.2959	0.9082	0.2959	$\pi/3$
3	4	0.9082	0.2959	0.2959	$\pi/3$
4	1	−0.2959	0.2959	0.9082	$\pi/3$
4	2	0.2959	0.2959	0.9082	$\pi/3$

as depicted in Fig. 1, the following equation is obtained:

$$\mu_{mn}(A_n I_n^{mn} - A_s I_s^{mn}) - (A_n - A_s)\frac{\alpha_{mn+1/2} I_P^{mn+1/2} - \alpha_{mn-1/2} I_P^{mn-1/2}}{w_{mn}} + Ar\xi_{mn}(A_e I_e^{mn} - A_w I_w^{mn}) = \tau_D(-I_P^{mn} + S)V_P \quad (9)$$

where the source term S is defined as

$$S = \frac{1-\omega_0}{\pi} T^4 + \frac{\omega_0}{4\pi}\sum_{m'}^{n_M}\sum_{n'}^{n_N} \Phi_{m'n' \to mn} w_{m'n'} I^{m'n'}. \quad (10)$$

To relate the facial intensities of the control volume and the edge intensities of the angular range to the cell centre intensity, the following linear equation is introduced:

$$I_P^{mn} = f I_{ic}^{mn} + (1-f) I_{is}^{mn} = f I_P^{mn+1/2} + (1-f) I_P^{mn-1/2}; \quad 1/2 \leqslant f \leqslant 1, \quad (11)$$

where subscript i represents the spatial direction r or z. The subscripts s and e denote the starting face from which a bundle of intensity originally comes, and the ending face at which the intensity arrives, respectively. For positive set of (μ_{mn}, ξ_{mn}), the subscripts s and e represent (s, n) along r-direction and (w, e) along z-direction individually. Rearranging equation (9) for I_P^{mn} and substituting equation (11) into the intensities for ending face and direction of $mn+1/2$ results in

$$I_P^{mn} = \frac{|\mu_{mn}|\bar{A}_r I_{rs}^{mn} + Ar|\xi_{mn}|\bar{A}_z I_{zs}^{mn} - \Gamma_{mn}\bar{\alpha}_{mn} I_P^{mn-1/2} + \tau_D f V_P S}{|\mu_{mn}|A_{re} + Ar|\xi_{mn}|A_{ze} - \Gamma_{mn}\alpha_{mn+1/2} + \tau_D f V_P}, \quad (12)$$

where the mean coefficients are defined as

$$\bar{A}_r = fA_{rs} + (1-f)A_{re}, \quad \bar{A}_z = fA_{zs} + (1-f)A_{ze},$$
$$\bar{\alpha}_{mn} = f\alpha_{mn-1/2} + (1-f)\alpha_{mn+1/2}, \quad \Gamma_{mn} = (A_n - A_s)/w_{mn}. \quad (13)$$

After finding the intensity at the cell centre, the intensities at the ending faces are calculated by using equation (11).

A numerical procedure starts by assuming that all the boundaries except the symmetric axis are black and no in-scattering term exists. With these assumptions the factor, f, is gradually increased globally from its initial value of 0.5 until the negative intensity is removed. When these physically unrealistic negative intensities appear, the real value of in-scattering is taken into account. The surrounding is taken to be black in this study, so all the radiant energy is absorbed therein. The global iterations are repeated until the solution converges.

The 41×22 nonuniform grid system is used, clustered near the boundary, because a steep temperature gradient would be established there. Due to a rapid change in early state, a variable time increment is adopted. The convergence is checked by a temperature difference between two iteration steps. The difference in two definitions of the mean emittance in equation (6) is another convergence criterion. A typical run requires about 8 s on the 80486 IBM PC compatible machine to get a converged solution for each time step.

4. RESULTS AND DISCUSSION

Numerical calculations were made for three parameters including the optical diameter, τ_D, conduction-to-radiation parameter, N, and scattering albedo, ω_0.

In Figs. 2(a) and (b), the transient radial temperature distributions at mid-plane and right end boundary are shown for two optical diameters. Since the medium is exposed to the rarefied cold environment, the internal energy of the cylindrical medium is rapidly decreasing due to the radiative heat loss at the boundary. As the medium cools down near the boundary, the temperature gradient is created therein. As time goes on, the position of the maximum tem-

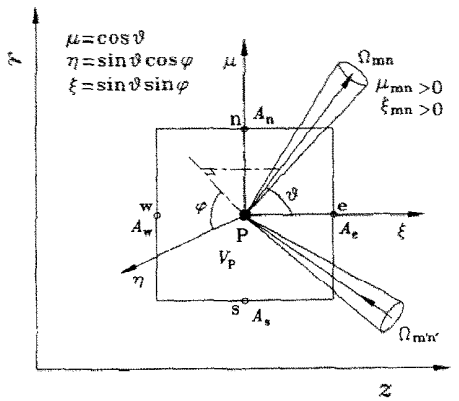

FIG. 1. Schematic of coordinate and grid system for computation.

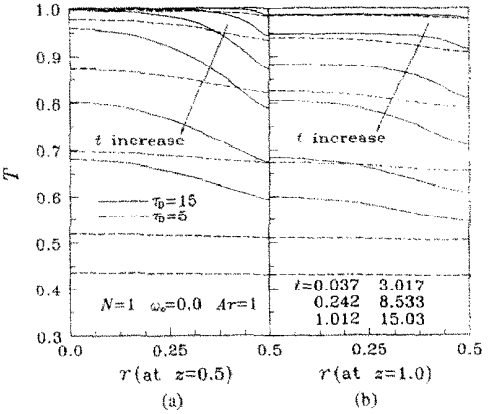

FIG. 2. Transient temperature profile: (a) at middle plane, (b) at right surface.

perature gradient migrates into the inner region with its value getting smaller, since the conduction plays a role inside the medium. This trend can be figured out in Fig. 3(a) where the conductive heat flux is plotted at various times. At the same time, the medium temperature becomes uniform as seen for $\tau_D = 5$ in the figure. As the cooling process goes further, the temperature gradually decreases maintaining its uniformity. The time interval between the onset of cooling and the establishment of the maximum temperature gradient is referred to as 'developing period' here. In this period the radiation is rather dominant over the conduction. And due to the radiative loss at the boundary, the steep temperature gradient is formed. Afterwards, there is also a period during which the conduction becomes more dominant than the radiation. In this interval the temperature distribution becomes uniform, for the conduction smoothens out the temperature gradient. This interval is named as 'relaxing period' here. This terminology is introduced here for simplicity of referring to its physical process.

Figure 2 also represents the effect of optical diameter, τ_D. The smaller τ_D, the faster the medium cools down and the more uniform the temperature distribution becomes. As τ_D gets smaller, the medium is well emitting the energy and the radiation can penetrate farther as shown in Fig. 3(b). Thus it can even influence the medium at long-distance and the temperature distribution is reduced uniform. Due to this far-reaching effect of the radiation, the medium can cool faster as τ_D is smaller.

Figure 4 illustrates a temporal variation of the dimensionless mean temperature and the mean emittance as defined in equations (5) and (6) for various values of τ_D. As τ_D decreases, the energy contained in inner side can be well transferred to the outer cold region by radiation. Therefore, the dimensionless mean temperature, which implies residual energy in the cylindrical medium, is lower for smaller τ_D during the entire cooling time. The mean emittance for $\tau_D = 5$

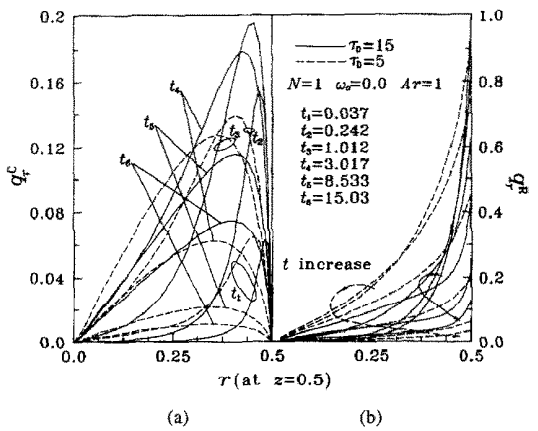

FIG. 3. Transient radial heat flux distribution at middle plane: (a) radial conductive heat flux, (b) radial radiative heat flux.

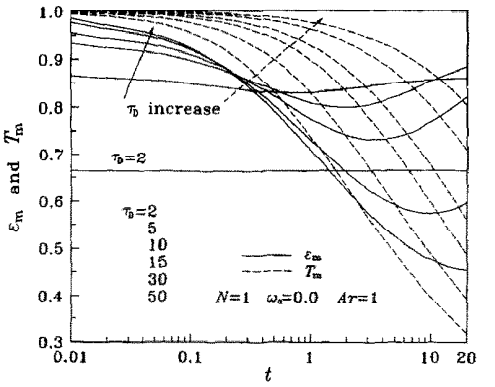

FIG. 4. Temporal variation of dimensionless mean temperature and mean emittance.

decreases for a while, since the rate of decrease of energy loss is smaller than the rate of decrease of mean temperature. Then after reaching its minimum, it increases. At this time the rate of decrease of energy loss is larger than the rate of decrease of mean temperature. As τ_D increases, this trend becomes more obvious and the time for minimal mean emittance is delayed, because less energy is lost through the boundaries, which is so called the heat blockage effect. In case for $\tau_D = 2$, even the energy kept in inner medium is easily radiated into the outside and the conduction redistributes energy inside the medium. This results in the rate of decrease of energy loss comparable to the rate of decrease of mean temperature. Therefore the mean emittance is kept nearly constant during the entire cooling period.

Figure 5 shows the temporal variation of isothermal contours for $N = 0.01$ and 1.0. Due to its symmetry only an upper right-hand half size of cylinder is displayed. It is seen that the region in contact with the cold environment starts to cool down. In the developing period the isothermal lines are located close together, in other words a steep temperature gradient is developed. Then, in the relaxing period the gap between the isothermal contours increases. This is previously explained with unsteady temperature gradient. In the case of $N = 1.0$ (dashed line in Fig. 5) there are fewer isothermal lines compared with $N = 0.01$ (solid line) and the gap between the isothermal contours is much larger. Physically the conduction plays a more significant role than the radiation, as N increases. So the energy can be more efficiently transferred in the medium. In other words the radiation results in the heat blockage effect.

Figure 6(a) shows a temporal variation of total radial heat flux at the radial middle plane for $N = 0.01$ and 1.0. Initially the total radial heat flux is almost the same regardless of N. However, as time passes, the total radial heat flux gets larger for larger N because of less heat blockage by radiation. A temporal change of the radiative heat flux at the circumferential surface is illustrated in Fig. 6(b). This flux is the energy lost

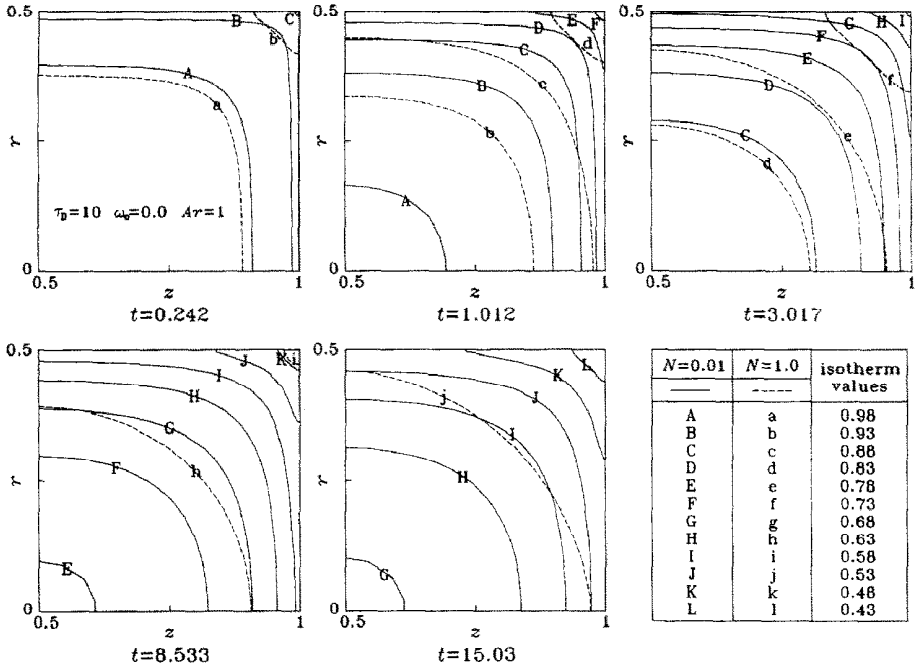

FIG. 5. Transient isothermal contours.

to the cold environment. As cooling progresses, more energy is lost for larger N for the same reason as aforementioned. But in the relaxing period almost the same amount of heat is irradiated at the boundary.

A transient change of the dimensionless mean temperature and the mean emittance for various values of N is represented in Fig. 7. As N increases, more energy is lost, which leads to smaller T_m. The mean emittance for fixed values of τ_D, ω_0 and Ar starts from the same initial value because the initial heat fluxes are all identical at the beginning. As N decreases, the redistribution of energy by conduction is less effective and so both developing and relaxing periods are prolonged. In a limiting case of $N = 0$, there is no relaxing period and a similar temperature profile, so-called fully developing condition, is obtained as described in the introduction. In the other limiting case of $N = \infty$ the uniform temperature is maintained during the whole cooling period, since heat dissipation by conduction is infinitely fast inside the medium.

In Figs. 8 and 9 the effect of the scattering albedo, ω_0, on the cooling characteristics is shown for fixed N, τ_D and Ar. The value of ω_0 is changing while β is kept constant. A transient change of temperature and radial heat flux along radial direction at the middle plane ($z = 0.5$) is represented in Figs. 8(a) and (b) for $\omega_0 = 0.1$ and 0.7. If ω_0 increases, the radiative emitting energy is reduced and is isotropically scattered in all directions with raised strength. Therefore, less energy is lost toward the boundary and energy

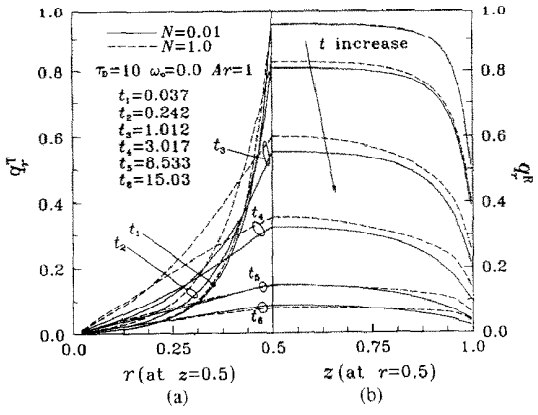

FIG. 6. Transient radial heat flux distribution: (a) total heat flux at middle plane, (b) total heat flux at circumferential surface.

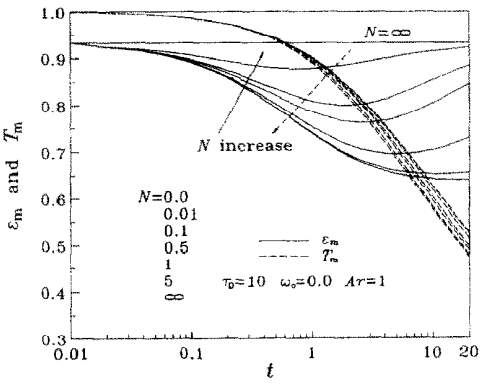

FIG. 7. Temporal variation of dimensionless mean temperature and mean emittance.

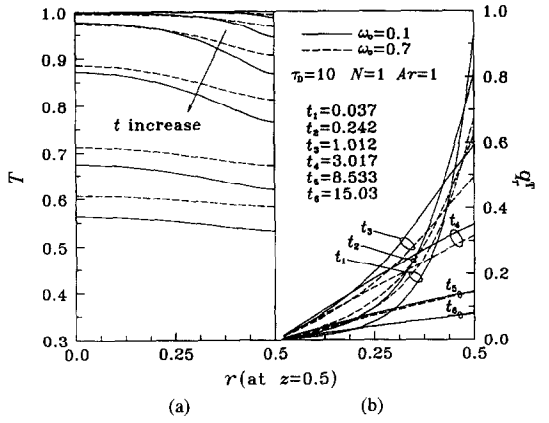

FIG. 8. Transient variation of temperature profile and radial total heat flux at middle plane: (a) temperature, (b) radial total heat flux.

sharing in the medium is favorable. This makes the rate of decrease of both temperature and radial heat flux smaller for $\omega_0 = 0.7$ in the figure.

In Fig. 9 the dimensionless mean temperature and the mean emittance are plotted with time for various values of ω_0. By the same reasoning described above, the mean temperature T_m is decreasing slower as ω_0 increases. Consequently less energy is lost to the cold environment, which also results in the smaller mean emittance for larger ω_0. In the case of $\omega_0 = 0.95$, a nearly constant mean emittance is obtained along the entire cooling time. Estimated from the curves for the mean emittance ε_m, an initially relatively small amount of heat is radiated to the surroundings for the large ω_0.

5. CONCLUSION

Using the finite difference technique with the Crank–Nicolson scheme to solve the energy conservation equation and applying the discrete ordinates method to the radiative transfer equation, the transient cooling of a cylindrical hot medium subjected to the rarefied cold environment has been analyzed in this work. Its cooling thermal characteristic have been investigated for three parameters including the optical diameter, τ_D, conduction-to-radiation parameter, N, and scattering albedo ω_0. The results obtained are as follows:

(1) As τ_D decreases, the cooling rate increases and the temperature profile tends to be uniform. Simultaneously, the developing period is shortened.

(2) As N decreases, the cooling rate decreases due to the heat blockage effect by radiation.

(3) As ω_0 increases, the cooling rate also decreases since less energy is emitted by the local medium and more energy is scattered inside the medium.

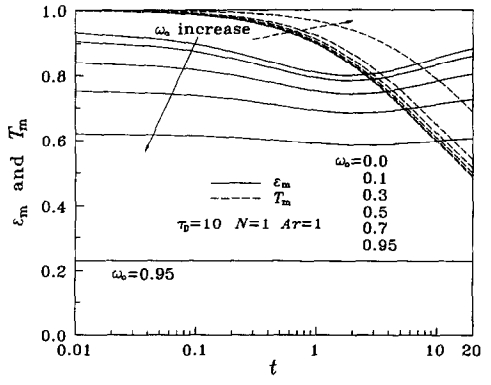

FIG. 9. Temporal variation of dimensionless mean temperature and mean emittance.

REFERENCES

1. Y. P. Chang and C. S. Kang, Transient and steady heat transfer in a conducting and radiating medium, *J. AIAA* **8**(4), 609–614 (1970).
2. D. G. Doornink and R. G. Hering, Transient combined conductive and radiative heat transfer, *J. Heat Transfer* **94**, 473–478 (1972).
3. K. C. Weston and J. L. Hauth, Unsteady, combined radiation and conduction in an absorbing, scattering, and emitting medium, *J. Heat Transfer* **95**, 357–364 (1973).
4. S. Kubo, Unsteady radiative heat transfer in a scattering-dominant medium, *J. AIAA* **22**(12), 1804–1809 (1984).
5. R. Siegel, Transient radiative cooling of a droplet-filled layer, *J. Heat Transfer* **109**, 159–164 (1987).
6. R. Siegel, Separation of variables solution for non-linear radiative cooling, *Int. J. Heat Mass Transfer* **30**(5), 959–965 (1987).
7. S. N. Tiwari and D. J. Singh, Transient energy transfer by conduction and radiation in nongray gases, *J. Thermophys.* **3**(2), 167–174 (1989).
8. T. H. Ping and M. Lallemand, Transient radiative–conductive heat transfer in flat glasses submitted to temperature, flux and mixed boundary conditions, *Int. J. Heat Mass Transfer* **32**(5), 795–810 (1989).
9. R. Siegel, Finite difference solution for transient cooling of a radiating–conducting semitransparent layer, *J. Thermophys.* **6**(1), 77–83 (1992).
10. F. Gordaninejad and J. Francis, A finite difference solution to transient combined conductive and radiative heat transfer in an annular medium, *J. Heat Transfer* **106**, 888–891 (1984).
11. R. Siegel, Transient radiative cooling of an absorbing and scattering cylinder—a separable solution, *J. Thermophys.* **2**(2), 110–117 (1988).
12. D. L. Ayers, Transient cooling of a sphere in space, *J. Heat Transfer* **92**(2), 180–182 (1970).
13. Y. Bayazitoglu and P. V. R. Suryanarayana, Transient radiative heat transfer from a sphere surrounded by a participating medium, *J. Heat Transfer* **111**, 713–718 (1989).
14. R. Siegel, Some aspects of transient cooling of a radiating rectangular medium, *Int. J. Heat Mass Transfer* **32**, 1955–1966 (1989).
15. R. Siegel, Transient cooling of a square region of radiating medium, *J. Thermophys.* **5**(4), 495–501 (1991).
16. B. G. Carlson and K. D. Lathrop, Transport theory—the method of discrete ordinates. In *Computing Methods in Reactor Physics* (Edited by H. Greenspan, C. N. Kelber and D. Okrent), pp. 165–266. Gordon & Breach, New York (1968).
17. A. S. Jamaluddin and P. J. Smith, Predicting radiative

transfer in axisymmetric cylindrical enclosures using the discrete ordinates method, *Combust. Sci. Technol.* **62,** 173–186 (1988).
18. W. A. Fiveland, Three-dimensional radiative heat-transfer solutions by the discrete-ordinates method, *J. Thermophys.* **2**(4), 309–316 (1988).
19. T. Y. Kim and S. W. Baek, Analysis of combined conductive and radiative heat transfer in a two-dimensional rectangular enclosure using the discrete ordinates method, *Int. J. Heat Mass Transfer* **34,** 2265–2273 (1991).
20. J. S. Kim, S. W. Baek and C. R. Kaplan, Effect of radiation on diffusion flame behavior over a combustible solid, *Combust. Sci. Technol.* **6**(2), 382–384 (1992).